J. Phys. D: Appl. Phys. **42** (2009) 195402 (5pp) doi:10.1088/0022-3727/42/19/195402

Structural and optical properties of N-doped ZnO nanorod arrays

Boqian Yang[1], **Peterxian Feng**[1,3], **Ashok Kumar**[1], **R S Katiyar**[1] **and Marc Achermann**[2]

[1] Department of Physics, University of Puerto Rico, Rio Piedras 00931, PR, USA
[2] Department of Physics, University of Massachusetts, Amherst, MA 01003, USA

E-mail: pfeng@cnnet.upr.edu and achermann@physics.umass.edu

Received 28 May 2009, in final form 24 July 2009
Published 14 September 2009
Online at stacks.iop.org/JPhysD/42/195402

Abstract
Large-scale arrays of N-doped ZnO nanorods have been synthesized on quartz substrates by pulsed laser deposition techniques. The ZnO/N nanorods have a diameter of 150–200 nm and a length of 1–1.5 μm. X-ray photoelectron spectroscopy analysis confirmed the implantation of nitrogen into the nanorod arrays and Raman scattering proved that their wurtzite structure was retained with high crystal quality. Optical spectroscopy showed that the incorporation of nitrogen into the ZnO nanorods reduced the transmission in the visible wavelength range. Room temperature and 4.6 K photoluminescence measurements of ZnO/N nanorods revealed intense UV peaks similar to ZnO and, at cryogenic temperature, a blue emission peak at 2.652 eV with a full width at half maximum of ∼83 meV.

(Some figures in this article are in colour only in the electronic version)

1. Introduction

One-dimensional (1D) ZnO nanostructures have attracted significant attention due to their potential applications in light-emitters [1], field-effect transistors [2] and gas sensors [3]. Various shapes of 1D ZnO nanostructures (nanorods, nanowires, nanobelts, nanorings, nanotubes, etc) have been fabricated in recent years by different techniques such as catalyst assisted thermal evaporation [4], non-catalytic thermal evaporation [5], wet chemical [6] and solvothermal/hydrothermal [7] route. However, the fabrication of high quality p-type ZnO nanostructures remains one of the challenges for the development of ZnO-based nano-devices. Surprisingly, very few reports demonstrated p-type doping of ZnO nanostructures using nitrogen, though initial fabrication methods of p-type ZnO thin films included N doping [8–11], due to its relatively shallow level [12]. Various types of nitrogen sources including N_2 [8], NH_3 [10], N_2O [11] and Zn_3N_2 [13] have been used depending on the growth techniques.

Although previous papers have reported the luminescence properties of p-typed ZnO/N [14–16], few of them have focused on ZnO/N nanostructures [9]. It has been shown that the photoluminescence (PL) emission of ZnO is composed of two parts: emission at the band edge in the UV region and defect-related deep-level emission in the green/yellow region [17]. In addition, very few reports demonstrated blue emission from ZnO nanostructures [18]. The origin of the blue emission is still controversial with several reported mechanisms [18, 19]. Cheng *et al* [18] suggested that the blue emission peak at 486 nm in ZnO tetrapodlike nanostructures is due to oxygen vacancies, which is the same mechanism that accounts for the green emission. Liu *et al* [19] reported that the blue emission at 435 nm in N-doped ZnO epilayers is related to impurity-induced defects caused by nitrogen incorporation.

In this paper, we report on the fabrication of ZnO/N nanorod arrays without catalyst and their optical properties. UV and blue emission of ZnO/N nanorod arrays are demonstrated.

2. Experimental details

Large-scale ZnO/N nanorod arrays were synthesized by pulsed laser deposition techniques in a nitrogen atmosphere. The experimental conditions were the same as those in our previous work [20], except after pumping the pressure of the chamber down to 10^{-6} Torr, nitrogen as working gas

[3] Author to whom any correspondence should be addressed.

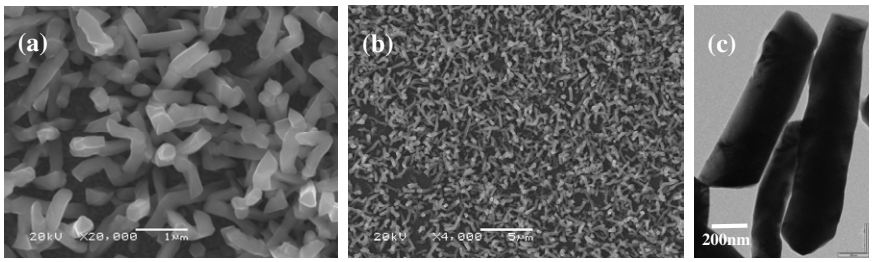

Figure 1. High (*a*) and low (*b*) magnification SEM images of ZnO nanorod arrays and TEM image (*c*) of individual nanorods.

was fed into the chamber up to a pressure of 400 mTorr. The duration of the deposition was 30 min, and the substrate temperature was kept at 350 °C. The morphology of the ZnO nanostructures was characterized by scanning electron microscopy (SEM), transmission electron microscopy (TEM) and the phase structures were tested by x-ray diffraction (XRD) with CuK_α radiation. The chemical bonds of these ZnO/N rods were examined using x-ray photoelectron spectroscopy (XPS) with an MgK_α x-ray source. Room temperature micro Raman scattering (RS) was performed using a Jobin-Yvon T64000 Triple-mate system with excitation at 514.5 nm by a coherent argon ion laser and a liquid nitrogen cooled CCD camera to collect and process the scattered data. The optical transmission spectra were recorded using an ultraviolet–visible spectrometer (Perkin-Elmer Model RS-2) in the range 300–900 nm. The PL was excited by frequency tripled pulses of a picosecond-mode Ti : sapphire oscillator (Coherent Mira) at a wavelength around 266 nm and detected with a thermoelectric cooled CCD camera. Low temperature measurements at 4.6 K were performed with a continuous flow liquid-He optical cryostat.

3. Results and discussion

Figures 1(*a*) and (*b*) show the top view of a ZnO/N nanorod array grown with a nitrogen pressure of 400 mTorr. The SEM picture displays a high density array of nanorods. The individual ZnO/N nanorods with diameters around 150–200 nm and lengths in the 1–1.5 μm range are shown in the TEM image of figure 1(*c*). The XRD pattern of the nanorod array is shown in figure 2. All peaks related to the hexagonal zinc oxide were identified and demonstrate (0 0 2) preferential orientation of the nanorods. The deposition at the nitrogen pressure of 400 mTorr yields a crystalline ZnO/N nanorod array with highly *c*-axis orientation.

The N concentration of ZnO/N nanorods was analysed by XPS. The full XPS spectrum of nanorods (figure 3(*a*)) showed peaks for no other elements than Zn, O, C and N. The C 1s peak is caused by the carbon tape used during the measurements. High-resolution XPS spectra of the Zn 2p and O 1s lines are shown in figures 3(*b*) and (*c*). The core lines of Zn 2p3/2 and 2p1/2 are located at 1022.80 eV and 1045.85 eV, respectively. No metallic Zn at 1021.50 eV was observed, which confirms that Zn exists only in the oxidized state [21]. The O 1s peak of ZnO/N nanorods splits into two peaks (figure 3(*c*)). The higher binding energy component located at 532.6 ± 0.2 eV is usually attributed to the presence of a $Zn(OH)_2$ phase in the

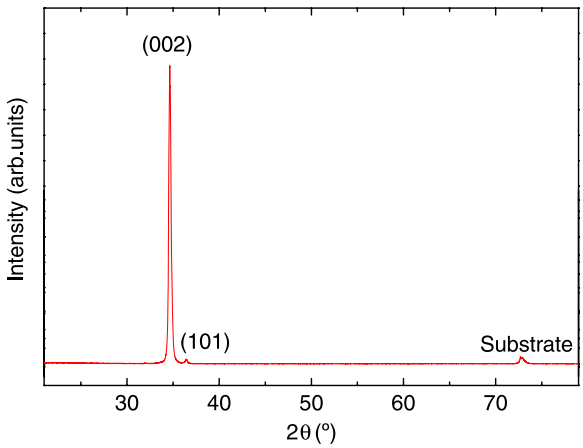

Figure 2. XRD of ZnO/N nanorod arrays prepared with nitrogen pressure of 400 mTorr on quartz substrates.

sample. This $Zn(OH)_2$ phase could be formed by absorbing atmospheric moisture [22]. The peak at 531.1 ± 0.2 eV can be due to the O–Zn bond formation, which is attributed to O^{2-} ions on the wurtzite structure of the hexagonal Zn^{2+} ion array [15]. In figure 3(*d*) we show that N 1s peaks at 397.7 eV, 400.4 eV and 407 eV are due to the formation of N_O–Zn, N–H and $(N_2)_O$–Zn bonds, respectively. Here, N_O is formed by substituting a single N atom for O and $(N_2)_O$ is formed when N_2 substitutes for an O atom in ZnO [23]. An oxygen-to-nitrogen atomic ratio of 4.4 : 1.0 is estimated by XPS, which indicates the formation of the ternary system of $ZnO_{0.815}N_{0.185}$, due to the high concentration of nitrogen in ZnO/N nanorods.

Micro-RS is very sensitive to the micro-structure of nanocrystalline materials [23], and it is used here to study the crystalline quality of the ZnO/N nanorod array. Figure 4 shows the Raman spectrum of the ZnO/N nanorods in comparison with that of a ZnO thin film prepared in vacuum with background pressure of 0.02 mTorr, but with other conditions identical. All six optical normal modes of ZnO are observed from the spectrum of ZnO/N nanorods. Peaks located at 98.1 cm^{-1}, 380.8 cm^{-1}, 410.0 cm^{-1} and 437.4 cm^{-1} correspond to E_2^{low}, A_1(TO), E_1(TO) and E_2^{high}, respectively [24]. The peak at 581.2 cm^{-1} can be assigned to the merging of A_1(LO) and E_1(LO) modes as shown in figure 4(b). This indicates that the ZnO/N nanorods and pure ZnO thin film keep the wurtzite crystal structure of the ZnO.

Apart from the ZnO normal optical modes of vibration, we observed four additive optical modes signed as A_1 (275.1 cm^{-1}), A_2 (329.4 cm^{-1}), A_3 (508.4 cm^{-1}) and A_4

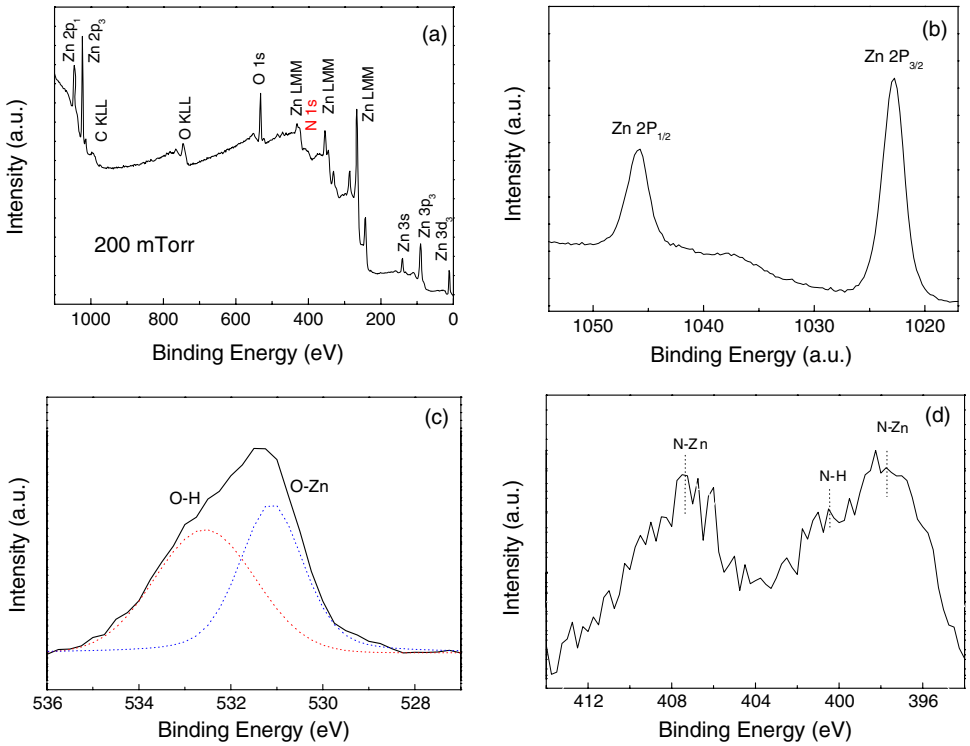

Figure 3. XPS spectra of ZnO/N nanorods: (*a*) full range survey spectrum, (*b*) Zn 2p spectrum, (*c*) O 1s spectrum and (*d*) N 1s spectrum.

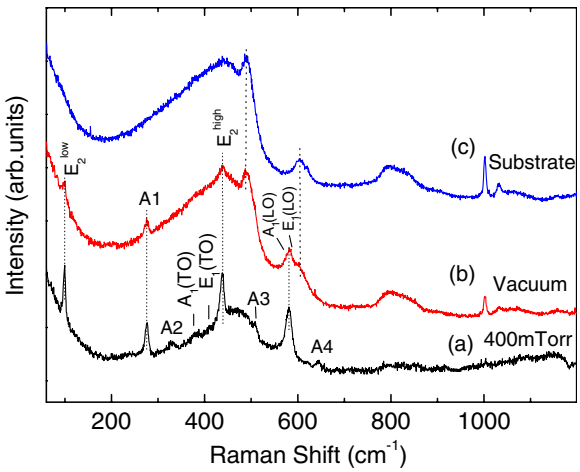

Figure 4. Room temperature Raman spectra: (a) ZnO/N nanorods prepared at nitrogen pressures of 400 mTorr, (b) ZnO thin film prepared in vacuum at background pressure of 0.02 mTorr and (c) the quartz substrate.

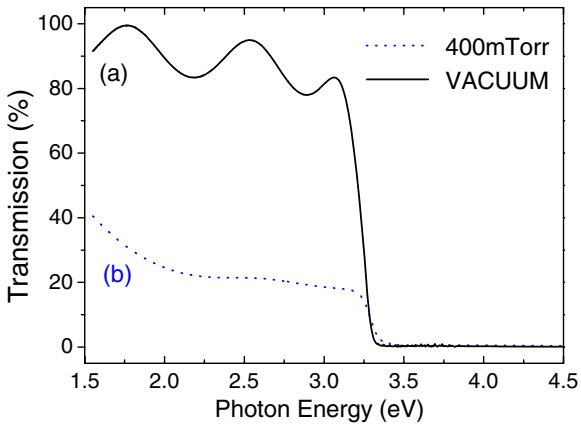

Figure 5. Optical transmission spectra of (a) pure ZnO thin film prepared in vacuum at background pressure of 0.02 mTorr and (b) ZnO/N nanorod array with nitrogen pressures of 400 mTorr.

(643.5 cm^{-1}) in figure 4. Different from the Raman frequencies excited in bulk of $Zn_{1-x}Mn_xO$ [25], the additive A_1 mode with high intensity is excited in either the ZnO/N nanorod or the pure ZnO film. This additive mode can be attributed to nanosize growths of nanorods or thin films, and explained as the contribution of zone phonon boundary [26]. According to [24], the additive modes of A_2, A_3 and A_4 are probably due to multiphonon processes, defects or impurities in ZnO/N nanorods. Compared with the pure ZnO thin film, five more Raman optical modes, A_2, A_1(TO), E_1(TO), A_3 and A_4, appear from ZnO/N nanorod samples that could result from the structural disorder of nanorods induced by the incorporation of N in the O site of the ZnO lattice. The structural disorder consequently drives the line width reduction of E_2 modes with the growth of ZnO/N nanorods as shown in figure 4.

Optical transmission spectra of the pure ZnO thin film and the ZnO/N nanorod array in the wavelength range from 250 to 800 nm are shown in figure 5. A sharp absorption edge at about 3.20 eV is observed for both samples. The spectral modulation in the pure ZnO thin film transmittance is caused by thin film interference. In the visible region of the transmittance spectra, an average transmission of >80% was measured, indicating good optical quality of the deposited film with low scattering or absorption losses. Compared with the transmission of the pure ZnO thin film, the transmission

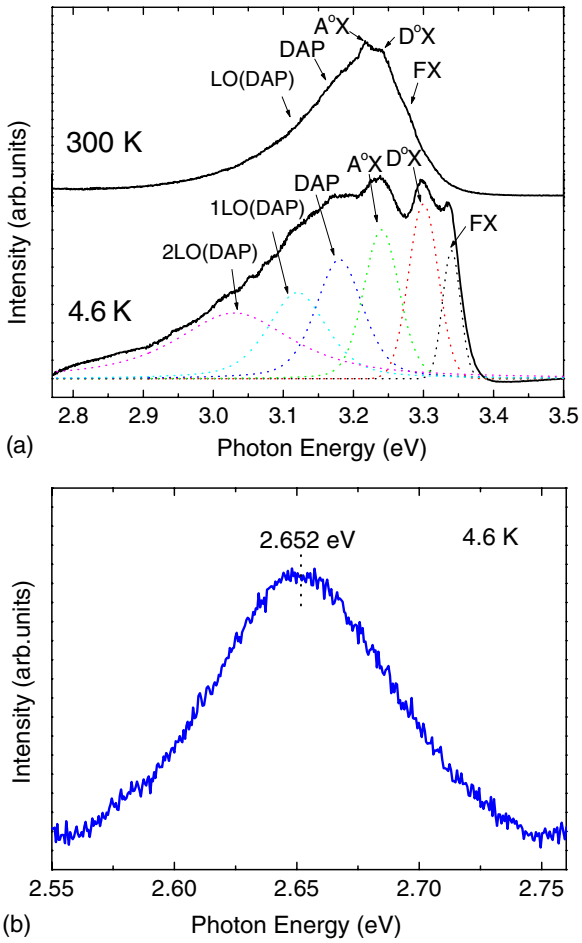

Figure 6. (*a*) Room temperature and 4.6 K PL spectra and (*b*) blue emission at 4.6 K of the ZnO/N nanorod array.

of the nanorod array (figure 5) in the visible range is much lower, because of diffuse scattering by the nanorod surface. The spectral interference fringes are less pronounced, which is likely due to the variations in nanorod length.

Figure 6(*a*) shows PL spectra of the ZnO/N nanorod array at room temperature and at 4.6 K. The room temperature PL spectra are characterized by a broad emission peak in the UV region with a full width at half maximum (FWHM) of 153 meV. As part of this emission peak, two shallow narrow peaks at 3.218 eV and 3.238 eV can be discerned that are probably attributable to acceptor-bound-excitons (A^oX) associated with the N_O acceptor and donor-bound-excitons (D^oX), respectively [27]. The broader shoulder on the lower energy side is due to donor–acceptor-pair (DAP) emission [27] and longitudinal optical-phonon (LO) replicas of the DAP band. The high-energy shoulder is assigned to free excitons (FX) [27]. Compared with pure ZnO nanorods [28] that show two strong band-edge PL peaks located at 3.29 and 3.34 eV, we observe a red-shift of the band-edge PL peaks of the doped ZnO/N nanorods. This red-shift can be explained by the substitution of oxygen with nitrogen in ZnO, which leads to a band bowing [29].

Employing low temperature measurements at 4.6 K allows us to clarify the band-edge PL peaks in the UV range (figure 6(*a*)). As expected, the lower temperature induces a general blue-shift of the dominant peaks. The peak frequencies are determined by a multi-Gaussian fit, and amount to 3.34 eV, 3.30 eV, 3.24 eV, 3.18 eV, 3.12 eV and 3.03 eV that correspond to the transitions FX, D^oX, A^oX, DAP, 1LO(DAP) and 2LO(DAP), respectively. Besides the UV emission, the 4.6 K PL spectrum of the ZnO/N nanorod array also shows a blue luminescence band, with a peak photon energy of 2.652 eV and a FWHM of ∼83 meV (figure 6(*b*)). Different from the origin of green luminescence [30], which is believed to be related to the defect of the oxygen/zinc vacancies, we attribute the appearance of the blue luminescence to nitrogen impurities implanted into the ZnO lattice. Further work is in progress in order to understand the origin and mechanism of blue emission from doped ZnO/N nanorod arrays.

4. Conclusions

In summary, large-scale N-doped ZnO nanorod arrays on quartz substrates have been fabricated by PLD in a nitrogen atmosphere. XPS confirms the implantation of N in ZnO with an oxygen-to-nitrogen ratio of ∼4.4 : 1.0. The structural disorder of ZnO/N nanorods induced by the incorporation of N is confirmed by additive multiphonon peaks in the RS spectra. Optical transmission spectra reveal that the transmission of the ZnO/N nanorod array decreases compared with pure ZnO thin films. The ZnO/N nanorod arrays luminesce at room and low temperature and one can easily discern between FX, D^oX, A^oX and DAP transitions. Interestingly, at low temperatures the PL spectra show a blue emission band centred at 2.652 eV that we attribute to transitions related to the nitrogen doping.

Acknowledgments

This work is partially supported by the NSF-EPSCoR fellowship, NSF-DMR (0706147) and DoD (W911NF-07-1-0014). The authors would like to thank Mr W Perez for assistance with the Raman measurements, Mr J Morales for SEM measurements, Mr Shojan Pavunny for transmission measurements, and Professor M Furis of the University of Vermont for the use of and support with the low temperature PL setup.

References

[1] Konenkamp R, Word R C and Schlegel C 2004 *Appl. Phys. Lett.* **85** 6004
[2] Park W I, Kim J S, Yi G-C, Bae M H and Lee H-J 2004 *Appl. Phys. Lett.* **85** 5052
[3] Kang B S, Ren F, Heo Y W, Tien L C and Norton D P and Pearton S J 2005 *Appl. Phys. Lett.* **86** 112105
[4] Huang M H, Mao S, Feick H, Yan H Q, Wu Y Y, Kin H, Weber E, Russo R and Yang P D 2001 *Science* **292** 1897
[5] Kar S, Pal B N, Chaudhuri S and Chakravorty D 2006 *J. Phys. Chem.* B **110** 4605
[6] Tian Z R R, Voigt J A, Liu J, Mckenzie B, McDermott M J, Rodriguez M A, Konishi H and Xu H F 2003 *Nature Mater.* **2** 821
[7] Dev A, Kar S, Chakrabarti S and Chaudhuri S 2006 *Nanotechnology* **17** 1533

[8] Iwata K, Fons P, Yamada A, Matsubara K and Niki S 2000 *J. Cryst. Growth* **209** 526
[9] Look D C, Reynolds D C, Litton C W, Jones R L, Eason D B and Cantwell G 2002 *Appl. Phys. Lett.* **81** 1830
[10] Ye Z-Z, Lu J-G, Chen H-H, Zhang Y-Z, Wang L, Zhao B-H and Huang J-Y 2003 *J. Cryst. Growth* **253** 258
[11] Guo X-L, Tabata H and Kawai T 2002 *J. Cryst. Growth* **237–239** 544
[12] Kobayashi A, Sankey O F and Dow J D 1983 *Phys. Rev. B: Condens. Matter* **28** 946
[13] Wang C, Ji Z, Liu K, Xiang Y and Ye Z 2003 *J. Cryst. Growth* **259** 279
[14] Zeuner A *et al* 2002 *Phys. Status Solidi* b **234** R7–9
[15] Gu Z B *et al* 2006 *Appl. Phys. Lett.* **88** 082111
[16] Tsukazaki A *et al* 2005 *Nature Mater.* **4** 42
[17] Yang B, Kumar A, Feng P and Katiyar R S 2008 *Appl. Phys. Lett.* **92** 233112
[18] Cheng W, Wu P, Zou X and Xiao T 2006 *J. Appl. Phys.* **100** 054311
[19] Liu W, Gu S L, Ye J D, Zhu S M, Liu S M, Zhou X, Zhang R, Shi Y and Zheng Y D 2006 *Appl. Phys. Lett.* **88** 092101
[20] Yang B, Kumar A, Zhang H, Feng P and Katiyar R S 2009 *J. Phys. D: Appl. Phys.* **42** 045415
[21] Islam M N, Gosh T B, Chopra K L and Acharya H N 1996 *Thin Solid Films* **280** 20
[22] Ghoshal T, Biswas S, Kar S, Dev A, Chakrabarti S and Chaudhuri S 2008 *Nanotechnology* **19** 065606
[23] Lee E C, Kim Y S, Jin Y G and Chang K J 2001 *Phys. B: Condens. Matter* **308** 912–5
[24] Damen T C, Porto S P S and Tell B 1966 *Phys. Rev.* **142** 570
Calleja J M and Cardona M 1977 *Phys. Rev.* B **16** 3753
[25] Samanta K, Dussan S, Katiyar R S and Bhattacharya P 2007 *Appl. Phys. Lett.* **90** 261903
[26] Yadav H K, Sreenivas K, Gupta V and Katiyar R S 2008 *J. Appl. Phys.* **104** 053507
[27] Ozgur U and Morkoc H 2006 Optical properties of ZnO and related alloys *Zinc Oxide Bulk, Thin Films and Nanostructures* ed C Jagadish and S J Pearton (Amsterdam: Elsevier) chapter 5 p 175
[28] Li S Z, Gan C L, Cai H, Yuan C L, Guo J, Lee P S and Ma J 2007 *Appl. Phys. Lett.* **90** 263106
[29] Persson C, Platzer-Bjorkman C, Malmstrom J, Torndahl T and Edoff M 2006 *Phys. Rev. Lett.* **97** 146403
[30] Lin B, Fu Z and Jia Y 2001 *Appl. Phys. Lett.* **79** 943
Lin B, Fu Z and Jia Y 2003 *Appl. Phys. Lett.* **82** 532